Linking River, Floodplain, and Vadose Zone Hydrology to Improve Restoration of a Coastal River Affected by Saltwater Intrusion

D. Kaplan and R. Muñoz-Carpena* University of Florida
Y. Wan, M. Hedgepeth, and F. Zheng South Florida Water Management District
R. Roberts and R. Rossmanith Florida Park Service

Floodplain forests provide unique ecological structure and function, which are often degraded or lost when watershed hydrology is modified. Restoration of damaged ecosystems requires an understanding of surface water, groundwater, and vadose (unsaturated) zone hydrology in the floodplain. Soil moisture and porewater salinity are of particular importance for seed germination and seedling survival in systems affected by saltwater intrusion but are difficult to monitor and often overlooked. This study contributes to the understanding of floodplain hydrology in one of the last bald cypress [*Taxodium distichum* (L.) Rich.] floodplain swamps in southeast Florida. We investigated soil moisture and porewater salinity dynamics in the floodplain of the Loxahatchee River, where reduced freshwater flow has led to saltwater intrusion and a transition to salt-tolerant, mangrove-dominated communities. Twenty-four dielectric probes measuring soil moisture and porewater salinity every 30 min were installed along two transects—one in an upstream, freshwater location and one in a downstream tidal area. Complemented by surface water, groundwater, and meteorological data, these unique 4-yr datasets quantified the spatial variability and temporal dynamics of vadose zone hydrology. Results showed that soil moisture can be closely predicted based on river stage and topographic elevation (overall Nash–Sutcliffe coefficient of efficiency = 0.83). Porewater salinity rarely exceeded tolerance thresholds (0.3125 S m^{-1}) for bald cypress upstream but did so in some downstream areas. This provided an explanation for observed vegetation changes that both surface water and groundwater salinity failed to explain. The results offer a methodological and analytical framework for floodplain monitoring in locations where restoration success depends on vadose zone hydrology and provide relationships for evaluating proposed restoration and management scenarios for the Loxahatchee River.

Coastal wetlands perform a unique suite of physical, biological, and chemical functions. They protect coastal areas from storm damage; filter, transform, and store sediments, nutrients, and other contaminants; and provide habitats that support huge numbers of commercially and ecologically important fish, birds, and other wildlife (e.g., Mitsch and Gosselink, 2000). Coastal zones also provide at least half of all global ecological services (Costanza et al., 1997) and generate billions of dollars annually from fisheries, recreation, and tourism (Niemi et al., 2004). Environmental pressures facing coastal wetlands come from natural and anthropogenic sources, and these stressors often overlap and have synergistic effects (McCarthy et al., 2001). Saltwater intrusion is an example of such a pressure.

Natural drivers of saltwater intrusion include climatic fluctuations that alter freshwater outflows (Thomson et al., 2001), storm surges and hurricanes (Flynn et al., 1995), and sea level rise (Moorhead and Brinson, 1995; Burkett et al., 2001). Estimated sea level rise alone has the potential to eliminate as much as 22% of the world's coastal wetlands by 2100 (Nicholls et al., 1999), although regional impacts would vary (Michener et al., 1997). Anthropogenic drivers of saltwater intrusion include land drainage (e.g., Holman and Hiscock, 1998); pumping of coastal freshwater aquifers (e.g., Sadeg and Karahanogulu, 2001); reduction in freshwater discharge from dam construction, water withdrawals, and other water diversions (e.g., Johnson, 1997); and hydraulic structures and land use changes within watersheds (e.g., Wang, 1988; Liu et al., 2001; Bechtol and Laurian, 2005). When anthropogenic and natural drivers act together, saltwater intrusion can lead to rapid and catastrophic loss of coastal wetlands (Wanless, 1989).

Saltwater intrusion in coastal wetlands causes plant stress or mortality from prolonged submergence or high salinities, erosion of wetland substrate, conversion of freshwater habitats to brackish or

J. Environ. Qual. 39:1570–1584 (2010)
doi:10.2134/jeq2009.0375
Published online 26 July 2010.
Received 23 Sept. 2009.
*Corresponding author (carpena@ufl.edu).

5585 Guilford Rd., Madison, WI 53711 USA

D. Kaplan and R. Muñoz-Carpena, Agricultural and Biological Engineering Dep., Univ. of Florida, 287 Frazier Rogers Hall, PO Box 110570, Gainesville, FL 32611-0570; Y. Wan, M. Hedgepeth, and F. Zheng, Coastal Ecosystems Division, South Florida Water Management District, 3301 Gun Club Road, West Palm Beach, FL 33406; R. Roberts and R. Rossmanith, Florida Park Service, Dep. of Environmental Protection 13798 SE Federal Highway, Hobe Sound, FL 33455.

Abbreviations: EC, electrical conductivity; ET, evapotranspiration; GWEC, groundwater electrical conductivity; MFL, minimum flows and levels; ppt, parts per thousand (salinity); RK, river kilometer; SFWMD, South Florida Water Management District; SWE, surface water elevation; SWEC, surface water electrical conductivity; T1, Transect 1; T7, Transect 7; VEC, valued ecosystem component; WTE, water table elevation.

saltwater habitats, and the transition of coastal saltwater habitats to open water (DeLaune et al., 1994). These effects have been observed in coastal wetlands around the globe, including the floodplain forests of the Mississippi River delta (Earles, 1975; Salinas et al., 1986), the coastal plains of the Mary and Alligator Rivers in northern Australia (Winn et al., 2004; Knighton et al., 1991), and the coastal marshes of the River Thurne in northeast Norfolk (UK) (Holman and Hiscock, 1998).

When saltwater intrusion is caused by anthropogenic drivers or by a combination of natural and anthropogenic drivers, some amount of restoration and management is likely achievable (Scruton et al., 1998). Re-establishing historical hydrological regimes and connections can ameliorate the effects of saltwater intrusion by increasing well-timed freshwater flows (Middleton, 2002) and, where appropriate, supplying the sediment required for accretion (DeLaune et al., 1994). Hydrological monitoring and modeling efforts in support of these restoration efforts usually focus on surface water (e.g., Wang, 1997) or groundwater (e.g., Jung et al., 2004) but overlook hydrological conditions in the vadose (unsaturated) zone, which largely dictate seed germination and seedling survival (Middleton, 1999). For example, the timing and duration of flooding and drawdown in the floodplain play a critical role in the reproduction of bald cypress [*Taxodium distichum* (L.) Rich.], a major component of floodplain swamps in 16 states in the United States (Thompson et al., 1999).

Along with water tupelo (*Nyssa aquatica* L.) and swamp tupelo (*Nyssa biflora* Walter), bald cypress is a dominant tree species in the riverine and coastal floodplains of the southeast (Day et al., 2006; Allen et al., 1994). Cypress seeds settle along drift lines after floodwaters recede and require moist but not flooded conditions to germinate (Middleton, 2000). Under saturated conditions, seeds may germinate on moss or wet muck but do not germinate under water, although they can remain viable for up to 30 mo if inundated (Fowells, 1965). At the other end of the moisture regime, seeds do not germinate on well-drained soils due to lack of surface moisture. Thus, a drawdown of inundated soils to saturated or moist conditions is required for germination (Burns and Honkala, 1990; Middleton 1999, 2002). Seedlings must also grow fast enough to keep their crowns above floodwaters for most of the growing season to survive (Conner, 1988; Conner and Toliver, 1987; Conner et al., 1986).

Bald cypress seeds and seedlings also have limited salt tolerance (Allen et al., 1996). The combined negative effects of flooding and salinity are greater than either alone and are more pronounced at higher salinities. In general, Chabrek (1972) found that bald cypress stands rarely occur naturally in areas with salinity exceeding 1.98 ± 1.40 (SD) parts per thousand (ppt), and Wicker et al. (1981) concluded that bald cypress forests are limited to areas where salinity does not exceed 2 ppt more than 50% of the time that trees are inundated. This is in agreement with Liu et al. (2006), who established a bald cypress seedling salinity tolerance threshold of 2 ppt using seedlings collected from the area studied in this paper. Given its specific life-cycle requirements, vadose zone hydrology is crucial to the maintenance and restoration of bald cypress floodplain swamp ecosystems

Like in many other states in the United States (e.g., Johnson, 2008), Florida law requires its water management agencies to establish Minimum Flows and Levels (MFLs) to protect water resources and valued ecosystem components (VECs) from "significant harm" (Section 373.042[1], Florida Statutes). Bald cypress swamp has been identified as a VEC in the floodplain of the Loxahatchee River, a coastal river in the southeastern United States where restoration efforts to ameliorate saltwater intrusion are being developed and tested. Minimum Flows and Levels and restoration plan development initiated intensive watershed and hydrodynamic modeling efforts to identify relationships between upstream flow and downstream salinity and suggested target MFL and restoration flows (South Florida Water Management District [SFWMD], 2002, 2006). However, these models focused primarily on the river channel and did not address the linkage with the vadose zone. The objective of this study was to develop relationships between surface water, groundwater, and vadose zone hydrology to better predict the effects of proposed restoration and management scenarios on ecological communities in the floodplain of the Loxahatchee River. This was achieved by long-term experimental characterization of soil moisture and porewater salinity dynamics in the floodplain at several depths and distances from the river—complemented by surface water and groundwater stage and salinity and meteorological monitoring—to identify differences between areas with varying soils, hydrology, and vegetation. It is the first effort of which we are aware that extends long-term, continuous hydrological monitoring into the vadose zone in support of wetland restoration.

Materials and Methods

Site Description

Historically part of the greater Everglades watershed, the Loxahatchee River is located on the southeastern coast of Florida, USA (26° 59′ N, 80° 9′ W) and is often referred to as the "last free-flowing river in southeast Florida" (SFWMD, 2006). The river has three main branches (the North, Southwest, and Northwest Forks), which join in a central embayment that connects to the Atlantic Ocean via Jupiter Inlet (Fig. 1). The watershed drains approximately 550 km^2 in Palm Beach and Martin Counties and includes several large, publicly owned areas including Jonathan Dickinson State Park (JDSP), the Loxahatchee Slough Preserve, and the J.W. Corbett Wildlife Management Area. In 1985 a 15.3-km stretch of the Northwest Fork became Florida's first National Wild and Scenic River (National Park Service, 2004).

The Northwest Fork of the Loxahatchee River (NW Fork) and its watershed contain a diverse array of terrestrial and aquatic ecosystems, including sandhill, scrub, hydric hammock (a plant community characterized by 30 to 60 d of inundation yearly and mixed, facultative hardwood species), wet prairie, floodplain swamp, estuarine (mangrove) swamps, seagrass beds, tidal flats, oyster beds, and coastal dunes (Roberts et al., 2006; Treasure Coast Regional Planning Council, 1999). Many of these ecosystems remain relatively intact (VanArman et al., 2005) and support a diversity of protected animal and plant species, including the endangered Florida manatee (*Trichechus manatus latirostris*) and four-petal pawpaw (*Asimina tetramera* Small) (SFWMD, 2006). The upper watershed of the NW Fork is also home to one of the last remnants of bald cypress floodplain swamp in southeast Florida. However, changing hydrology and salinity

regimes in the river and its floodplain have been linked to vegetative changes in the floodplain forest (SFWMD, 2002). Of primary concern are (i) the transition from bald cypress floodplain swamp to mangrove-dominated communities in the tidal floodplain as salinity increased and (ii) inadequate hydroperiod in the upstream riverine floodplain, which has shifted the system toward drier plant communities (SFWMD, 2009). Similar changes in the composition of floodplain vegetation as a result of reduced flooding frequency have been observed regionally and globally (e.g., Darst and Light, 2008; Leyer, 2005).

Altered hydroperiods and encroaching salinity in the NW Fork have been linked to the following four major factors: (i) construction of major and minor canals that direct water away from the historic watershed; (ii) the permanent opening of Jupiter Inlet in 1947 (Fig. 1); (iii) construction of the C-18 canal in 1958, which transferred a majority of flow from the NW Fork to the Southwest Fork (Fig. 1); and (iv) lowering of the regional groundwater table by municipal withdrawals (SFWMD, 2002). These hydrologic changes have been linked to changes in the vegetative composition of the floodplain, where studies have documented the upriver retreat of bald cypress since at least the turn of the 20th century (General Land Office, 1855; Alexander and Crook, 1975; McPherson, 1981; Roberts et al., 2008, Ward and Roberts, unpublished observation).

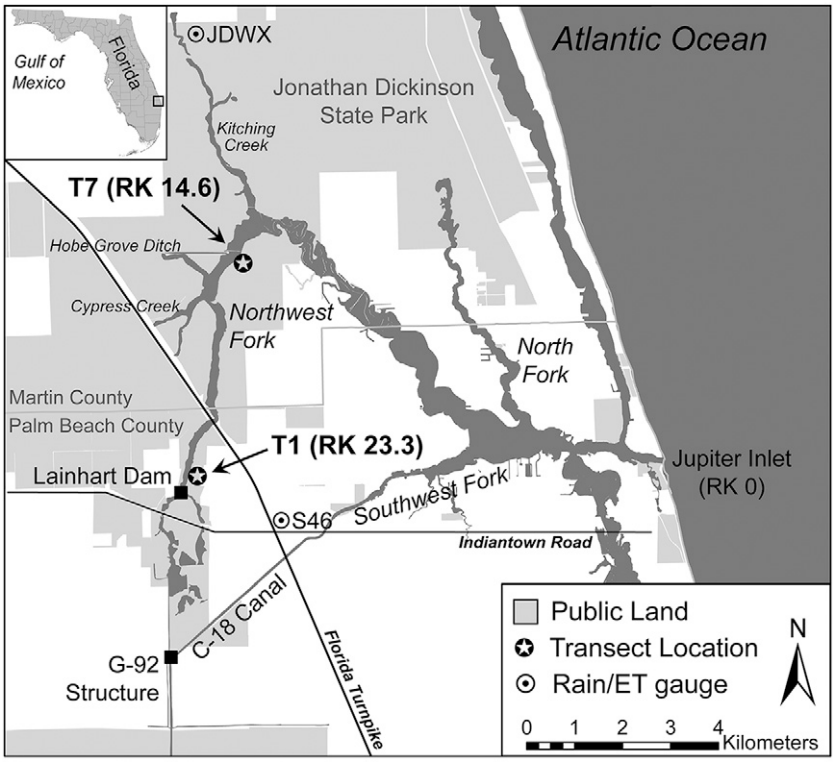

Fig. 1. The Loxahatchee River and surrounding area with transect locations (T1/T7), meteorological measurement locations (S46 and JDWX weather stations) and major hydraulic infrastructure. Transect notation is followed by distance from river mouth. ET, evapotranspiration; RK, river kilometer.

Based on interpretation of aerial photography (SFWMD, 2002), in 1940 mangroves were dominant as far as 9.7 km upstream of the river mouth (indicated as river kilometer [RK] 9.7) and extended upstream to RK 12.5 (Fig. 2a). Bald cypress floodplain swamp communities were present upstream of RK 10.5 and were dominant above RK 12.9. By 1995, large areas of mangroves had been destroyed due to urbanization in the lower section of the river (Fig. 2b). However, mangrove-dominated communities had replaced bald cypress as far upstream as RK 16.9, and upstream bald cypress–dominated swamp had transitioned to shorter-hydroperiod freshwater swamp (with bald cypress present but declining). Only minor changes in vegetative coverage were observed between 1985 and 1995, likely due to increased flows after a 1982 consent decree between the Florida Wildlife Federation and the SFWMD (SFWMD, 2006).

The MFL for the NW Fork of the Loxahatchee River (SFWMD, 2002) was adopted in 2003, and a restoration plan (SFWMD, 2006) was completed in 2006 with the goal of protecting the river's remaining cypress swamp and hydric hammock communities, as well as estuarine resources including oysters (*Crassostrea virginica*), fish larvae, and sea grasses—all identified as VECs. These MFL and restoration scenarios rely primarily on increased freshwater flow over Lainhart Dam (Fig. 1), which was found to be the most important driver of upstream hydroperiod and downstream surface water salinity (SFWMD, 2006). Despite the Loxahatchee's "free-flowing" appellation, flow over Lainhart dam (calculated from headwater surface water elevation) is controlled by managing conveyance through the G-92 water control structure (Fig. 1).

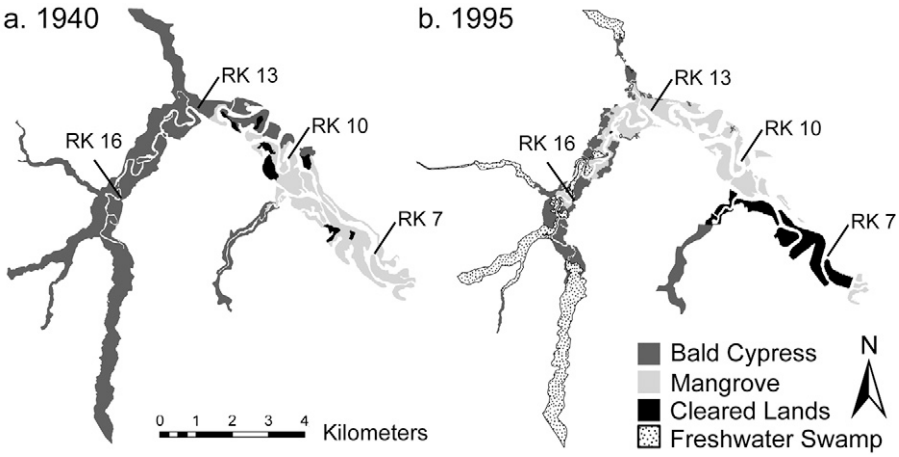

Fig. 2. Interpretation of aerial photography of vegetation communities in the floodplain of the Northwest Fork of the Loxahatchee River in (a) 1940 and (b) 1995. Distance upstream from river mouth is denoted by river kilometer (RK). By 1995, mangroves had displaced large areas of bald cypress in the lower and middle sections of the river due to saltwater intrusion. Bald cypress were present, but declining, in upstream freshwater swamp due to reduced hydroperiod. Adapted from SFWMD (2002) (data acquired from SFWMD staff).

Experimental Setup

Twenty-four frequency domain reflectometry dielectric probes (Hydra Probe; Stevens Water Monitoring Systems, Beaverton, OR) measuring soil moisture, bulk electrical conductivity, and temperature were installed at four locations and three depths along two previously established vegetation survey transects perpendicular to the river (Fig. 3). Probe installation elevations were determined using established survey benchmarks and a rotary self-leveling laser (model LM500; CST/Berger, Watseka, IL). Each cluster of three probes was wired to a field data logger (CR10/CR10-X, Campbell Scientific, Logan, UT), which recorded data every 30 min. Every 2 to 4 wk, system batteries were changed, and data were downloaded to a laptop. Data collection began in September 2004 at Transect 1 and in January 2005 at Transect 7 and continued through September 2008.

Transect 1 (T1) is in an upstream, riverine area (RK 23.3; Fig. 1) not affected by daily tides and has elevations ranging from 4.19 to 1.66 m in the river channel (Fig. 3a) (elevations are referenced to the National Geodetic Vertical Datum of 1929 [NGVD29]). Soils on the higher elevation hydric hammock consist of Winder fine sand, transitioning to sandy clay loam at depths of ~90 cm (Mortl, 2006). In the lower floodplain, soils are classified as fluvents— stratified entisols made up of interbedded layers of sand, clay, and organic matter, typical of areas with frequent flooding and deposition (Sumner, 2000)—with sand content increasing with depth (Mortl, 2006). This freshwater transect contains hydric hammock at higher elevations and mature bald cypress swamp (average diameter at breast height, 49 cm) at lower elevations. Invasion of less flood-tolerant species into the hydric hammock and riverine floodplain in this and other upstream areas has been documented (SFWMD, 2009), indicating the ecological impact of shortened hydroperiod.

Transect 7 (T7) is in a downstream, transitional area (RK 14.6; Fig. 1) that receives daily tidal flooding of varying salinity over most or all of its length and has elevations ranging from 3.07 m in the upland to 0.40 m in the floodplain (Fig. 3b). Soil on T7 is a highly organic muck (Terra Ceia Variant muck) (Soil Survey Staff, 1981) with depths of over 1 m, underlain by sand (Mortl, 2006). Vegetation studies indicate that this transect has been affected by saltwater intrusion, logging, and invasion by exotic plants (SFWMD, 2006). Transect 7 contains a mix of floodplain swamp communities representing a gradient of decreasing salinity tolerance with increasing distance from the river. From the river's edge to approximately 30 m inland, floodplain vegetation is classified as upper tidal swamp dominated by red mangrove (*Rhizophora mangle* L.), which is highly salt tolerant. With increasing distance from the river, this community transitions to mixed tidal swamp dominated by pond apple (*Annona glabra* L.), which is moderately salt tolerant (~30 to 75 m from the river); riverine mixed swamp, which includes a mix of flood-tolerant hardwoods dominated by bald cypress, pond apple, wax myrtle (*Myrica cerfiera* L.), pop ash (*Fraxinus caroliniana* Mill.), and sabal palm [*Sabal palmetto* (Walter) Lodd. Ex Schult. & Schult. f.] (~75 to 110 m from the river); and riverine swamp, which is dominated by bald cypress and pop ash (110–140 m from the river) (SFWMD, 2009) (Fig. 3b).

Dielectric Probe Principles and Operation

The Hydra frequency domain reflectometry dielectric probe determines soil moisture and electrical conductivity (EC) by measuring soil dielectric properties. Dielectric permittivity (ε) is related to the dielectric constant (K), and the permittivity of free space (ε_o) by

$$\varepsilon = K\varepsilon_o \quad [1]$$

$$K = \varepsilon_r - i\varepsilon_i \quad [2]$$

where K is a complex number composed of real (ε_r) and imaginary (ε_i) dielectric constants (Campbell, 1990). The Hydra probe generates a 50-MHz electromagnetic wave, most of which is absorbed by the soil. The portion of the wave that reflects creates a standing wave, which characterizes K. The probe measures four analog voltage outputs: three to calculate ε_r and ε_i based on K and one to calculate soil temperature. Temperature-corrected (25°C) ε_r is used to calculate volumetric soil moisture (θ), and temperature-corrected ε_i is used to calculate bulk soil EC

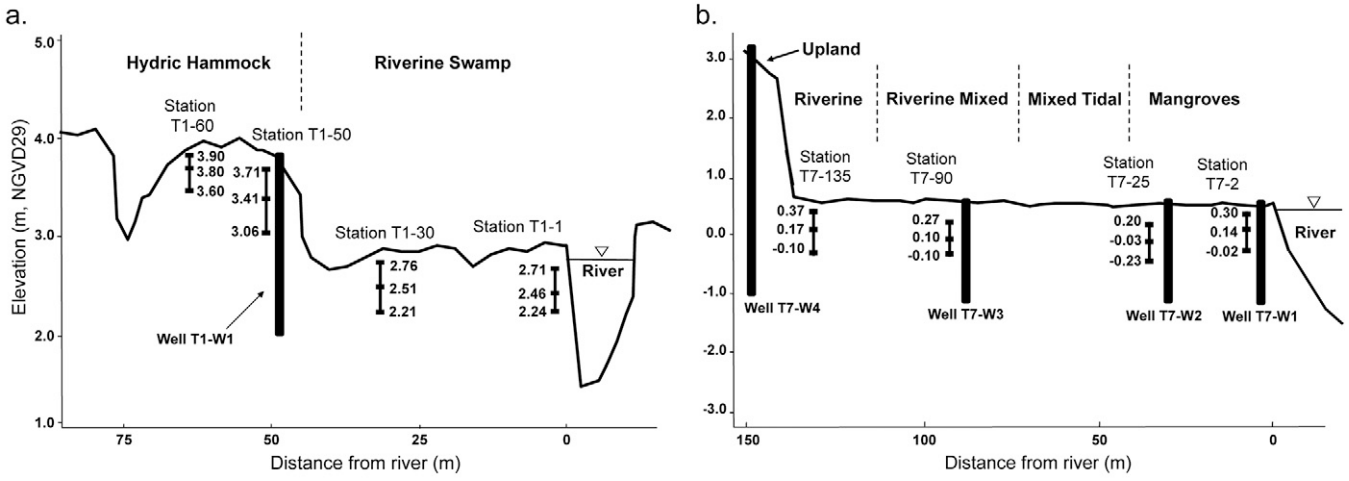

Fig. 3. Topography, layout of vadose zone monitoring stations and groundwater wells, and dominant vegetation communites on (a) Transect 1 and (b) pore Transect 7. Station names denote transect number (T1/T7) and distance from the river (m). Probe installation elevations (m, NGVD29) are listed below each station.

(σ_b). Finally, σ_b and θ are used to calculate porewater EC (σ_w). Calculations of θ, σ_b, and σ_w were based on Hydra probe calibrations developed specifically for the soils of the Loxahatchee River floodplain by Mortl (2006).

Unlike synoptic weekly or monthly sample collection, automated, continuous, 30-min monitoring of θ and σ_w using dielectric probes allowed us to investigate vadose zone hydrodynamics over different time scales (from storm event, to tidal cycle, to seasonal and interannual variation). In contrast to soil sample collection for moisture analysis and extraction of porewater for chemical analysis, this method did not require soil disturbance except during initial probe installation (and replacement, when necessary). Finally, unlike field studies of saltwater intrusion into coastal aquifers, which focus on groundwater EC in the saturated zone (e.g., Melloul and Goldenberg, 1997), the use of dielectric probes in this study allowed us to observe changes in root zone EC under inundated, saturated, and unsaturated conditions while also providing soil moisture data.

Meteorological, Surface Water, and Shallow Groundwater Data

Average annual precipitation in the Loxahatchee River watershed is 155 cm yr^{-1}, with approximately two thirds falling during the wet season from May to October (Dent, 1997). In southern Florida, average annual evapotranspiration (ET) losses are 114 cm yr^{-1} (SFWMD, 2002). For this study, rainfall data were recorded at the S46 hydraulic structure on the Southwest Fork, and ET data were recorded at the JDWX weather station in JDSP (Fig. 1). These data are publicly available and were downloaded from the SFWMD online environmental database, DBHYDRO (Stations S46_R and JDWX; http://my.sfwmd.gov/dbhydroplsql/).

Surface water elevation (SWE) and surface water EC (SWEC) were recorded at two stations in the NW Fork close to Transects 1 and 7. A SFWMD monitoring station on the headwater side of Lainhart Dam (0.45 km upstream of T1) measured average daily SWE and is available on DBHYDRO (station LNHRT_H; Fig. 1). The Loxahatchee River District (LRD) maintains a water quality monitoring station (datasonde station 69) on the NW Fork at Indiantown Road that measured SWEC hourly (Fig. 1; data acquired from LRD staff). A United States Geological Survey (USGS) monitoring station in the river at RK 14.6 (adjacent to T7) measured SWE and SWEC every 15 min (Station ID: 265906080093500; data acquired from USGS staff; station funded by SFWMD).

Finally, the SFWMD and Florida Park Service installed and monitored 12 shallow groundwater wells in the floodplain of the NW Fork, including four on T7 and one on T1 (Fig. 3). In general, the ~500-m shallow aquifer in the area is made up of sand, limestone, and shell beds and is separated from the deeper Floridan aquifer by ~100 m of low permeability clay (Toth, 1987). However, the groundwater data presented in this study were collected in the top 1 to 5 m to assess possible shallow groundwater effects on floodplain vegetation. Wells were constructed of slotted 5.08-cm (nominally 2-in) PVC pipe housed in a 20.32-cm (nominally 8-in) PVC pipe, and were backfilled with 20/30 silica sand filter pack from 15.24 cm (nominally 6 in) below the bottom of the well to 60.96 (nominally 2 ft) above the top of the well screen. A 15.24-cm layer of 30/65 fine sand and 15.24 cm of bentonite clay were placed above the filter pack, and the well was finished with Portland Type I neat cement grout to 15.24 cm below the top of well risers, which rose 91.44 cm (nominally 3 ft) above the ground surface. Screen size was 0.254 mm (nominally 0.01 in). Water table elevation (WTE) and groundwater electrical conductivity (GWEC) data were measured every 30 min using TROLL 9000/9500 multiparameter water quality probes (In-Situ Inc., Ft. Collins, CO), and were analyzed in Muñoz-Carpena et al. (2008). Table 1 summarizes well attributes.

Soil Moisture–Surface Water Elevation Relationships

Soil moisture time series for each probe are presented as actual (measured) soil moisture using a soil-specific calibration. However, Mortl (2006) found the soils in the Loxahatchee River floodplain to fall into three distinct groups with widely varying hydrologic characteristics: sand, found primarily on the higher elevation hydric hammock on T1; fluvent, found in the floodplain on T1; and muck, found in the floodplain of T7 (Table 2). Thus, when comparing θ across soil categories it was helpful to normalize θ using effective soil moisture, which scales values from zero to unity and is calculated by

$$\Theta_e = \frac{\theta - \theta_r}{\theta_s - \theta_r} \quad [3]$$

where Θ_e is effective soil moisture content (–),θ is the actual (measured) soil moisture content ($m^3\ m^{-3}$), θ_r is the residual soil moisture content ($m^3\ m^{-3}$), and θ_s is the saturated soil moisture content ($m^3\ m^{-3}$). Relationships between Θ_e and SWE were then explored at each transect.

For the 12 measurement locations at upstream T1, average daily Θ_e in the floodplain versus average daily SWE was fit to a common model (sigmoid, two parameters) of the form:

$$\Theta_e = \frac{1}{1 + e^{-\left(\frac{SWE - a}{b}\right)}} \quad [4]$$

Table 1. Locations and attributes of the five groundwater wells in the study. Wells are distributed across two transects (T1 and T7). River kilometer indicates distance from the river mouth. Well elevation denotes elevation at the ground surface.

Well	Transect type	River kilometer	Distance from river	Well elevation	Screened elevation
			m	m, NGVD29	
T1-W1	riverine	23.3	50	3.28	1.51 to 2.12
T7-W1	transitional	14.6	2	0.36	–1.49 to –0.88
T7-W2			30	0.43	–1.40 to –0.79
T7-W3			90	0.56	–1.13 to –0.52
T7-W4			130	2.94	–0.73 to 0.79

Table 2. Characteristics of the three Loxahatchee River floodplain soil categories described by Mortl (2006).

Soil category	ρ_b†		K_s‡		θ_r§	θ_s§	%C¶	
	Mean ± SD	Range	Mean ± SD	Range			Mean ± SD	Range
	g cm^{-3}		cm h^{-1}					
Sand	1.36 ± 0.18	1.06–1.55	37.04 ± 7.70	29.26–48.42	0.04	0.40	0.45	0.10–0.48
Fluvent	0.69 ± 0.38	0.30–1.22	84.33 ± 83.52	0.81–166.17	0.20	0.90	11.0	1.0–15.0
Muck	0.25 ± 0.15	0.14–0.54	3.05 ± 2.29	0.23–7.18	0.20	0.90	20.0	5–25

† Field bulk density.

‡ Saturated hydraulic conductivity.

§ Residual (θ_r) and saturation (θ_s) soil moisture.

¶ Percent carbon.

where SWE is measured at Lainhart Dam (m, NGVD29), and *a* and *b* are curve parameters. The Nash–Sutcliffe coefficient of efficiency ($-\infty \le C_{eff} \le 1$) (Nash and Sutcliffe, 1970) was used as a measure of goodness-of-fit. A general model and nomograph for Θ_e on T1 were then developed by investigating trends between the *a* and *b* parameters in Eq. [4] and probe installation elevations, depths, and distances from the river. This resulting model was used to evaluate Θ_e profiles across T1 under different management scenarios.

At downstream T7, daily tidal flooding resulted in a limited range of θ near θ_s for all probes. However, responses to brief periods of drawdown in the shallowest (i.e., highest elevation) soils on T7 were evaluated using Fast Fourier Transform smoothing (Press et al., 1993) of 15- and 30-min θ and SWE data to investigate correlation between the series.

Surface Water, Groundwater, and Porewater Electrical Conductivity Relationships

Based on output from hydrodynamic and salinity models (RMA-2 and RMA-4) (USACE, 1996), the SFWMD (2006) developed regression equations for downstream surface water salinity at 15 sites in the NW Fork versus freshwater flow of the form:

$$Y = Y_0 + ae^{-bx} \quad [5]$$

where *x* is total freshwater flow (ft^3 s^{-1}) to the NW Fork from Lainhart Dam and from three tributaries (Kitching Creek, Cypress Creek, and Hobe Grove Ditch; Fig. 1); *Y* is salinity (ppt); and Y_0, *a*, and *b* are parameters. The predictive ability of this model was tested at RK 14.6 (adjacent to T7) using flow and SWEC data observed over the 4-yr field study. Freshwater flow requirements to maintain SWEC below the 2 ppt bald cypress salinity threshold (equivalent to an EC of 0.3125 Siemens per meter [S m^{-1}] at 25°C [Richards, 1954]) were also identified based on measured data. Finally, σ_w values were compared with SWEC and GWEC at each transect and with the 0.3125 S m^{-1} threshold to (i) explore relationships between the series; (ii) determine the number of days that this threshold was exceeded in surface water, groundwater, and porewater; and (iii) assess the likelihood that MFL and restoration scenarios will adequately control σ_w in the floodplain.

Results and Discussion

Global Descriptive Statistics

Despite difficult field conditions (hurricanes, frequent lightning strikes, inundation in saline water, equipment damage by insects and other animals, bioturbation of soil by plant roots and burrowing animals), frequent field visits ensured data completeness over the 4-yr study period with few gaps, with over 1.5 million measurements collected from the 24 dielectric probes (time series completeness ranged from 73 to 99.9%; average, 85%). Minimum, maximum, and average daily θ and σ_w for the 24 measurement locations are summarized in Table 3. Sandy soils on the hydric hammock on T1 (stations T1-60 and T1-50) had the lowest and most variable θ, with values observed over a large range of moisture contents. On the other hand, θ was higher (at or near θ_s) and less variable in the floodplain of T1 (stations T1-30 and T1-1) and over the entire length of T7 (stations T7-135, T7-90, T7-25, and T7-2). The θ_s values were highest in the organic, low ρ_b muck and fluvent soils but were variable within soil "groups," especially for the fluvent soil in the floodplain at T1, which had variable and alternating layers of sand, clay, and organic matter.

Probe calibrations for σ_w as a function of σ_b and θ do not hold under low soil moisture conditions (Hilhorst, 2000), so σ_w was not calculated for the highest elevation soils on T1, which often had θ < 0.10. However, average σ_b values measured in these soils were the lowest in the study ($0.001 \le \sigma_b \le 0.003$ S m^{-1}), suggesting that σ_w is not a concern in this area. Maximum daily average σ_w over the 4-yr study (0.220 S m^{-1}) was observed at upstream station T1-1, which is above the influence of daily tides. Maximum 30-min σ_w (0.596 S m^{-1}) was recorded at downstream station T7-25, which receives daily tidal flooding.

The hydrological data collected during this study represent a wide range of climatic conditions, including four wet/dry seasonal cycles, two wet years with hurricane-induced flooding (2004–2005), and the driest 2-yr period (2006–2007) recorded in south Florida since 1932 (Neidrauer, 2009). The dynamics (magnitude, duration, and timing) of θ and σ_w variation, and how these variables relate to rainfall, surface water, and groundwater, are explored further in Fig. 4 and 5 and sections below.

Hydrological Time Series

Upstream Transect 1

Figure 4 shows selected hydrological time series collected on or near upstream T1. Large rainfall events coincided with peaks in SWE and WTE series, which were closely correlated (r^2 = 0.93) during wet seasons (Fig. 4a). During dry periods, SWE at Lainhart Dam remained relatively level close to the dam overflow elevation due to the impoundment, and flow over the dam (~0.5 m^3 s^{-1}, about one half of the MFL) was insufficient to keep the floodplain

at T1 hydrated. Water table elevation at T1 fell below SWE measured at Lainhart Dam in each of the four dry seasons observed, driven by ET and low rainfall (most drastically in 2006 and 2007). However, SWE data measured adjacent to the transect from July to December 2008 (SFWMD, unpublished data; not shown) showed that WTE at T1 was always greater than the adjacent SWE during this period, indicating that the NW Fork likely has consistent gaining stream conditions in this location.

Surface water elevation and WTE dynamics were reflected in θ time series (Fig. 4b and 4c), especially in the highest elevation soils on T1. For example, large θ peaks in surface soils in 2005 corresponded to intense rainfall events (and attendant increases in SWE and WTE) associated with three tropical storms that passed over the experimental area in July, September, and October of that year (Fig. 4b, solid line). Variation in θ was damped for middle elevation soils, but effects of environmental conditions (rain, SWE, and WTE) were still apparent (Fig. 4b, dashed line). The lowest elevation (i.e., deepest) soils experienced long periods of saturation (Fig. 4b, dotted line). Even at this depth, soils dried down to θ_r for long periods during the dry seasons of 2005, 2006, and 2007. This frequently dry soil profile in the hydric hammock root zone helps explain the invasion of upland plant species such as slash pine (*Pinus elliottii* Engelm.) and the exotic Caesar-weed (*Urena lobata* L.) into the hydric hammock observed in SFWMD (2009).

In the lower floodplain, θ was less variable, although surface soils experienced considerable drying during all dry seasons (most markedly in 2006 and 2007; Fig. 4c, solid line). Although θ values between 0.5 and 0.7 would not be considered "dry" in a mineral soil, they corresponded to very dry conditions at the soil surface of the highly organic and clayey soils in the floodplain at T1. Under these moisture conditions, soil shrank away from tree trunks, and facultative wetland plant species like sabal palm, Hottentot fern [*Thelypteris interrupta* (Willd.) K. Iwats.], and the exotic wild taro [*Colocasia esculenta* (L.) Schott] invaded the floodplain (SFWMD, 2009), competing with floodplain species for water, light, nutrients, and space. Overly dry surface soils are also unfavorable for bald cypress seed germination (Middleton, 1999). Even when surface soils were resaturated by fall (when cypress seeds drop), the area for successful seed germination was reduced by the invasion of facultative and upland species during previous dry-downs. Lower elevation soils in the floodplain on

Table 3. Summary of experimental data from the 24 probes on Transect 1 (T1, upstream) and Transect 7 (T7, downstream). Probe naming convention indicates transect number (T1/T7), distance from the river (m), and probe elevation (m, NGVD29). Monitoring began in September 2004 at stations T1-60 and T1-50; in January 2005 at stations T1-30, T1-1, T7-135, and T7-90; and in May 2005 at stations T7-25 and T7-2 and continued through September 2008.

Probe	*N*†	θ‡		σ_w§	
		Mean ± SD	Range	Mean ± SD	Range
		$m^3\ m^{-3}$		S m^{-1}	
Transect 1—hydric hammock/riverine swamp					
T1-60 (3.90 m)	69169	0.06 ± 0.05	0.01–0.41§	—¶	—¶
T1-60 (3.80 m)	69077	0.13 ± 0.09	0.02–0.50	—¶	—¶
T1-60 (3.60 m)	69004	0.24 ± 0.11	0.01–0.40	—¶	—¶
T1-50 (3.71 m)	72765	0.11 ± 0.08	0.02–0.56	—¶	—¶
T1-50 (3.41 m)	72681	0.22 ± 0.13	0.03–0.45	—¶	—¶
T1-50 (3.06 m)	72739	0.29 ± 0.08	0.07–0.38	0.052 ± 0.011	0.000–0.099
T1-30 (2.76 m)	67061	0.70 ± 0.06	0.56–0.76	0.089 ± 0.057	0.000–0.210
T1-30 (2.51 m)	66970	0.75 ± 0.02	0.71–0.79	0.128 ± 0.044	0.000–0.205
T1-30 (2.21 m)	66917	0.74 ± 0.01	0.71–0.77	0.091 ± 0.007	0.078–0.110
T1-1 (2.71 m)	65446	0.80 ± 0.07	0.56–0.91	0.220 ± 0.063	0.114–0.412
T1-1 (2.46 m)	63948	0.77 ± 0.03	0.71–0.82	0.124 ± 0.029	0.072–0.229
T1-1 (2.24 m)	67057	0.66 ± 0.01	0.62–0.69	0.153 ± 0.015	0.110–0.193
Transect 7—mixed freshwater and mangrove swamps					
T7-135 (0.37 m)	65447	0.80 ± 0.05	0.75–0.90	0.065 ± 0.069	0.000–0.379
T7-135 (0.17 m)	65447	0.83 ± 0.05	0.75–0.88	0.043 ± 0.054	0.000–0.285
T7-135 (−0.10 m)	65448	0.78 ± 0.02	0.75–0.81	0.007 ± 0.017	0.000–0.091
T7-90 (0.27 m)	65565	0.77 ± 0.02	0.74–0.84	0.131 ± 0.058	0.040–0.287
T7-90 (0.10 m)	64998	0.79 ± 0.02	0.75–0.86	0.121 ± 0.037	0.057–0.273
T7-90 (−0.10 m)	64124	0.77 ± 0.02	0.75–0.81	0.120 ± 0.048	0.042–0.332
T7-25 (0.20 m)	61006	0.80 ± 0.03	0.75–0.86	0.094 ± 0.098	0.000–0.596
T7-25 (−0.03 m)	60956	0.82 ± 0.04	0.75–0.90	0.109 ± 0.087	0.024–0.553
7-25 (−0.23 m)	61009	0.82 ± 0.03	0.75–0.91	0.104 ± 0.087	0.020–0.501
T7-2 (0.30 m)	60062	0.77 ± 0.03	0.75–0.83	0.114 ± 0.101	0.018–0.556
T7-2 (0.14 m)	56569	0.77 ± 0.02	0.75–0.79	0.123 ± 0.093	0.018–0.480
T7-2 (−0.20 m)	57375	0.75 ± 0.01	0.75–0.77	0.103 ± 0.078	0.021–0.337

† Number of data points.

‡ Soil moisture.

§ Porewater electrical conductivity.

¶ Calibration for σ_w does not hold at low θ, however average bulk soil EC (σ_b) was extremely low in these soils.

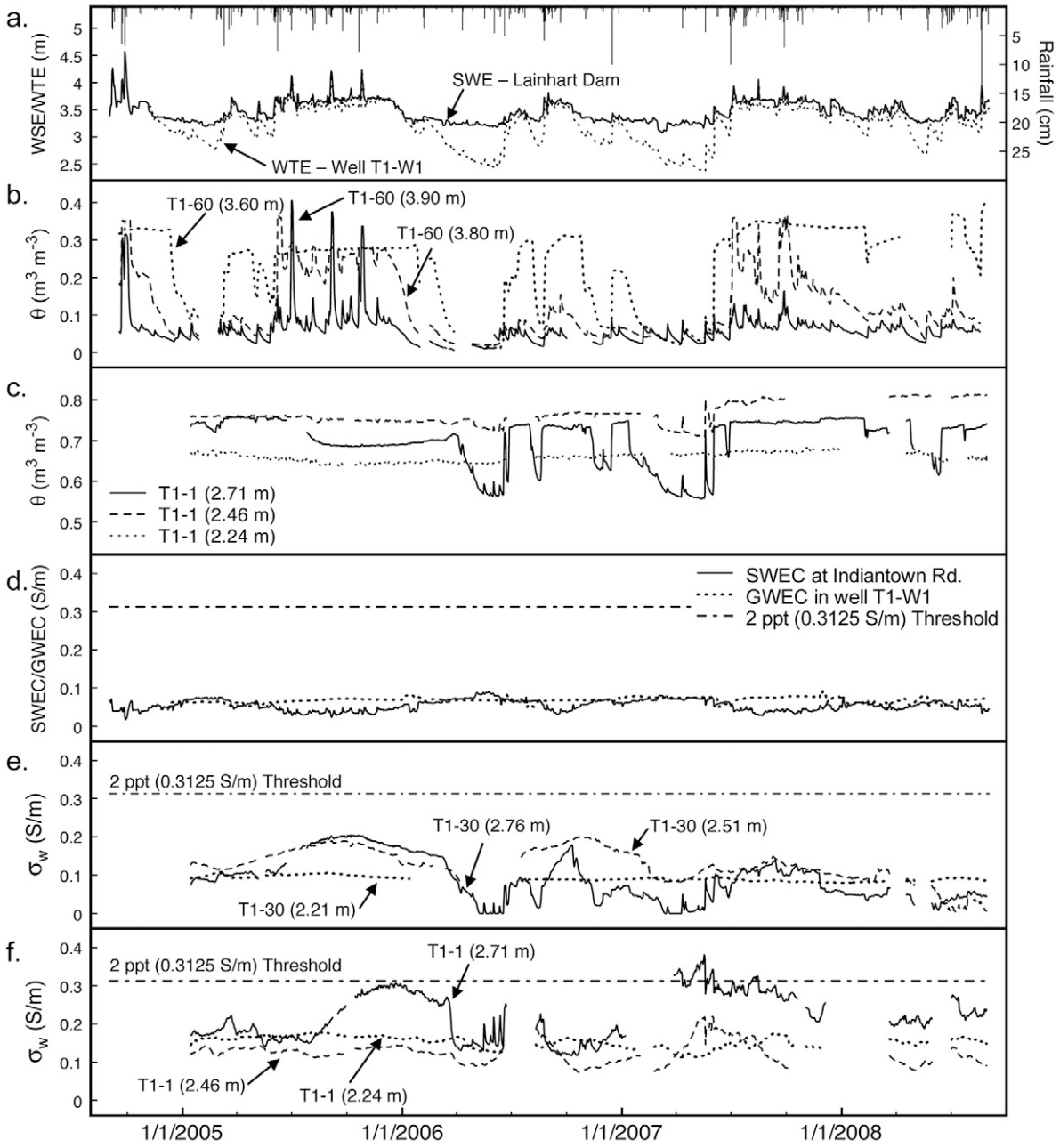

Fig. 4. Precipitation, surface water elevation (SWE), water table elevation (WTE), soil moisture (θ), surface water and groundwater electrical conductivity (SWEC and GWEC), and soil porewater electrical conductivity (σ_w) measured at selected stations on or near upstream Transect 1. Naming of vadose zone data series (θ and σ_w) indicates transect number (T1/T7), distance from river (m), and probe installation elevation (m, NGVD29). Gaps in time series represent missing data.

T1 remained consistently saturated, though at slightly different values of θ_s due to the heterogeneity of soil layering in the floodplain (Fig. 4c, dashed and dotted lines). This suggests that mature trees with developed root systems experienced little or no water stress.

On T1, SWEC and GWEC were low and had similar magnitudes (average of 0.054 and 0.068 S m^{-1}, respectively), remaining well below the 0.3125 S m^{-1} threshold over the entire study period (Fig. 4d). In the floodplain, σ_w was consistently higher than SWEC and GWEC (by a factor of 2–3 times) (Fig. 4e and 4f), although no consistent relationships between σ_w and other hydrological or meteorological variables were found. Values of σ_w were highest in the surface soils closest to the river and exceeded the 0.3125 S m^{-1} threshold (though slightly) for 59 d in 2007 (Fig. 4f, solid line). Based on the data recorded in this study, it is unlikely that σ_w reaches high enough levels to cause acute salt stress to bald cypress on T1, even during extended dry periods. It may cause chronic stress for shallow-rooted, salt-sensitive species, however, which could be ameliorated by more frequent, longer-duration inundation of the floodplain by the adjacent (low EC) surface water (Richardson and Hussain, 2006; Abrol et al., 1988).

Downstream Transect 7

Figure 5 shows selected hydrological time series collected on or near downstream T7. Surface water elevation at downstream

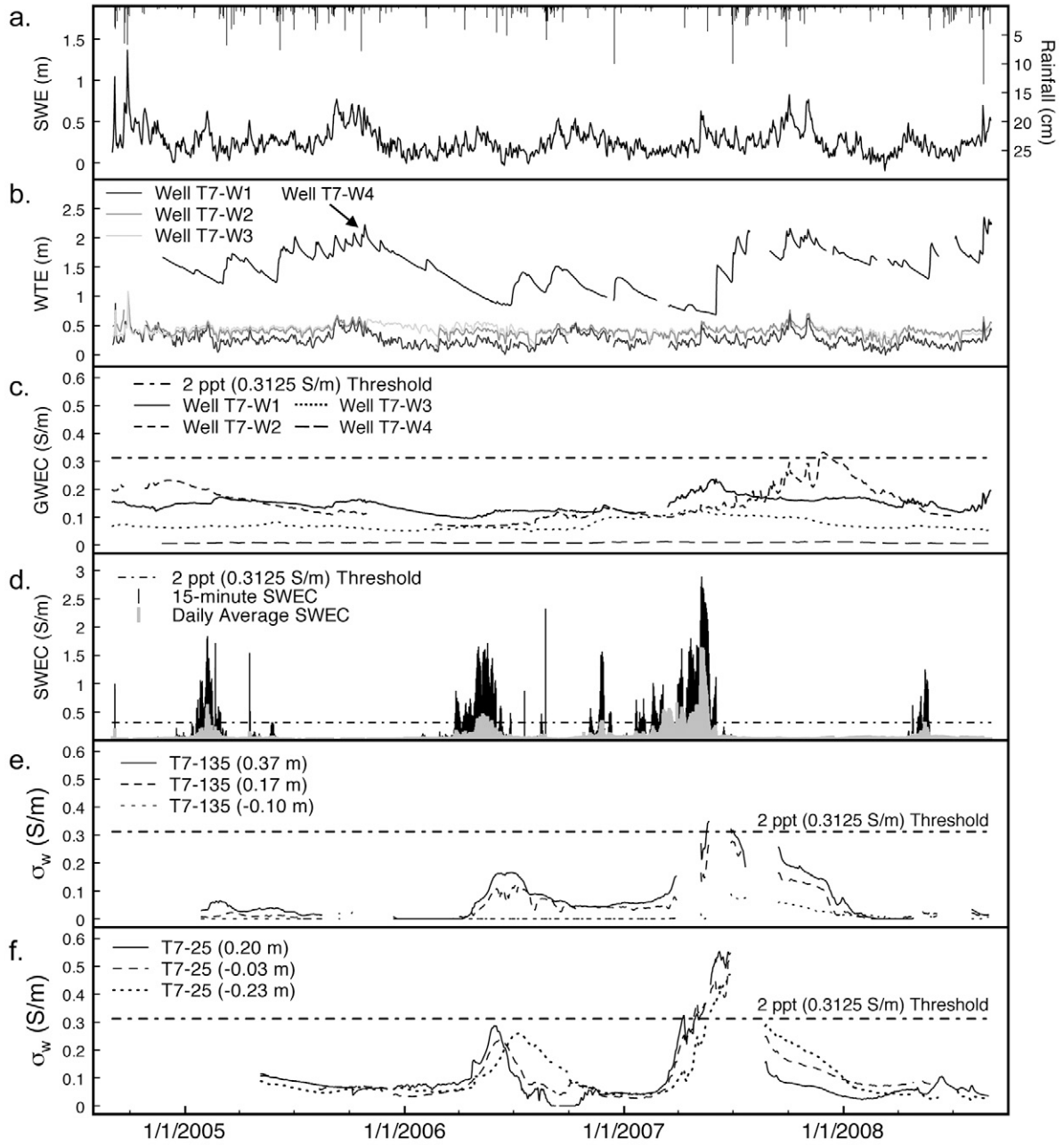

Fig. 5. Precipitation, surface water elevation (SWE), water table elevation (WTE), surface water and groundwater electrical conductivity (SWEC and GWEC), and soil porewater electrical conductivity (σ_w) measured at selected stations on or near downstream Transect 7. Naming of vadose zone data series (σ_w) indicates transect number (T1/T7), distance from river (m), and probe installation elevation (m, NGVD29). Gaps in time series represent missing data.

T7 is influenced primarily by daily and monthly tidal cycles, although high water events may also be associated with storm surges and large rainfall events. For example, high SWE in September 2004 was caused by tidal surge and increased freshwater flow in the NW Fork during Hurricanes Frances and Jeanne, which passed over the study site (Fig. 5a). Water table elevation in the upland well on T7 (T7-W4; Fig. 5b, dark line) showed responses to wet and dry season rainfall patterns similar to those observed in upstream SWE and WTE. During the dry seasons of 2006 to 2007, WTE in this well fell considerably but remained higher than WTE in floodplain wells (Fig. 5b, lower lines), which were lower (close to mean sea level) and more influenced by daily tidal oscillations. This indicates a variable but consistently positive flow of freshwater from the uplands to the river through the floodplain, even under extreme drought conditions.

Upland well T7-W4 had the lowest GWEC on T7 (Fig. 5c, lower dashed line). This low GWEC, combined with the maintenance of high WTE in the upland, likely plays a role in regulating σ_w and GWEC in the floodplain, mitigating the severity of saltwater intrusion at this transect. Groundwater EC was generally highest closest to the river and decreased with distance toward the upland, although this trend reversed in 2007, when GWEC in well T7-W2 surpassed that of well T7-W1 for the duration of the year before falling in 2008 (Fig. 5c). Groundwater EC approached the 0.3125 S m^{-1} threshold only briefly at the end of 2007 in well T7-W2, several months after peaks in SWEC and σ_w (Fig. 5d–5f). Based on these data, it is

unlikely that groundwater directly contributes to increases in the σ_w observed on this transect; instead, GWEC shows a damped and delayed response to high-EC surface water.

Peaks in SWEC at T7 occurred in four distinct periods corresponding to dry seasons with low rainfall and low upstream SWE (Fig. 5d), although the peak was earlier in 2005 (centered around March) than in other years (centered around May). Surface water EC, measured at 15-min intervals, reached maxima of 1.250 to 2.890 S m^{-1} during the dry seasons of 2005 to 2008 (4 to 9 times the 0.3125 S m^{-1} threshold). Because SWEC at RK 14.6 varied over a tidal cycle, daily average SWEC maxima were lower (~1 to 5 times the threshold) but still exceeded the threshold for 6 d in 2005, 18 d in 2006, and 64 d in 2007.

Peaks in σ_w corresponding to SWEC were observed across T7 during each dry season (Fig. 5e-f). At station T7-135 (farthest from the river), peaks in σ_w increased in magnitude from 2005 through 2007 but reached the critical limit only for a brief period in 2007 and only in the highest-elevation soils (Fig. 5e, solid line). The lowest-elevation soils at this station (Fig. 5e, dotted line) had low σ_w throughout the measurement period, similar in magnitude to GWEC in upland well T7-W4 (Fig. 5c). Despite repeated SWEC peaks at RK 14.6, σ_w in the soil profile 135 m from the river remained relatively low. Time series of σ_w from station T7-90 (not shown) were similar to those at station T7-135, with σ_w approaching the critical value only in the dry season of 2007.

Station T7-25 is closer to the river, where vegetation transitions to salt-tolerant mangroves (Fig. 3b). Here σ_w was higher (Fig. 5f), exceeding the critical value for a considerable time in 2007 (53, 55, and 34 d in the surface, middle, and lower probe elevations, respectively, not including days during a gap in data). Linear interpolation of the σ_w trend during this data gap yields an estimate of 83, 85, and 64 d in 2007 when σ_w exceeded the critical threshold at the three measurement elevations. Data from station T7-2 (not shown) closely mirrored the timing and magnitude of σ_w data from station T7-25 but had slightly lower σ_w and longer lags (up to 90 d) between SWEC and σ_w peaks in the lowest-elevation soils.

Table 4 summarizes the duration of SWEC, GWEC, and σ_w exceedances on T7 from 2005 to 2008. Surface water EC exceeds the 0.3125 S m^{-1} limit for extended periods of time in three of the four study years but does not explain the distribution of variably salt-tolerant vegetation across the transect because the entire floodplain is inundated twice daily by tidal flooding. Although GWEC generally decreased with increasing distance from the river, it was lower than the critical salinity threshold at all locations on all but 3 d of the 4-yr study period and thus also failed to explain the observed vegetation patterns. On the other hand, the 12 σ_w data series described EC dynamics at the interface between surface water and groundwater (i.e., in the vadose zone) and showed that σ_w in the soil profile was above the critical limit 2 and 25 m from the river (where vegetation is dominated by salt-tolerant mangroves) but below the limit 90 and 135 m from the river (where vegetation consists of riverine and mixed swamps, dominated by bald cypress and pop ash [Fig. 3b]). This suggests that σ_w dynamics help to explain the distribution of variably salt-tolerant species across the floodplain, which neither SWEC nor GWEC were able to do.

Table 4. Number of days that the 2 ppt (0.3125 S m^{-1}) bald cypress salinity tolerance threshold was exceeded in porewater, surface water, and groundwater at Transect 7. Vadose zone monitoring stations and groundwater wells in which electrical conductivity did not exceed 0.3125 S m^{-1} in any year are excluded.

	Days threshold exceeded			
	2005	2006	2007	2008
Porewater				
T7-135 (0.37 m)	0	0	26	0
T7-90 (–0.10 m)	0	0	6	0
T7-25 (0.20 m)	0	0	83	0
T7-25 (–0.03 m)	0	0	85	0
T7-25 (–0.23 m)	0	0	64	0
T7-2 (0.30 m)	0	0	113	0
T7-2 (0.14 m)	0	0	51	0
T7-2 (–0.2 m)	0	0	9	0
Surface water				
RK 14.6	6	18	64	0
Groundwater				
T7-W2	0	0	3	0

Finally, T7 has very little variation in elevation and received tidal inundation over most or all of its length nearly every day. Thus, θ values on this transect were relatively constant at or near θ_s and are not shown.

Surface Water–Soil Moisture Relationships

Upstream Transect 1

Average daily θ in the floodplain of T1 was scaled to Θ_e, plotted against average daily SWE at Lainhart Dam, and fit to the common sigmoid model given in Eq. [4] (Fig. 6) with good results (overall C_{eff} = 0.92 for the 12 measurement locations).

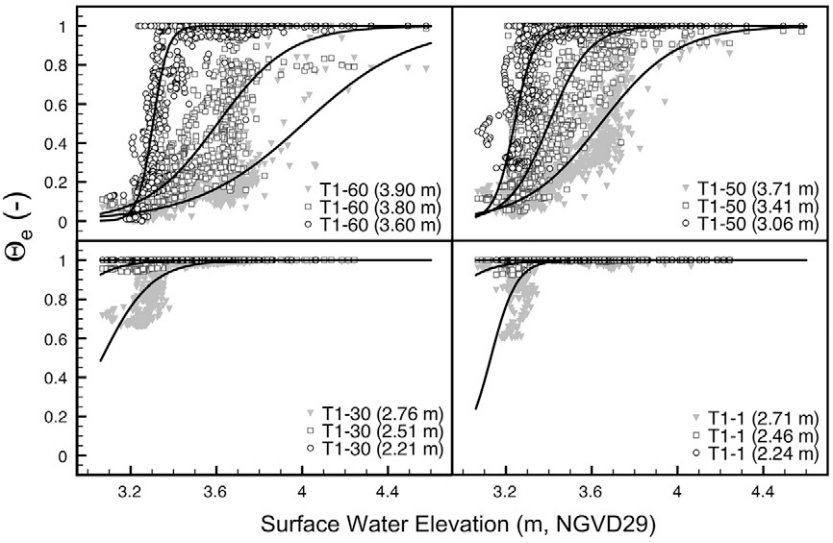

Fig. 6. Observed (symbols) and modeled (lines) effective soil moisture (Θ_e) versus surface water elevation at Lainhart Dam for the 12 monitoring locations on Transect 1.

Values of θ_s for the three soil groups given in Mortl (2006) were based on composite soil samples and did not represent the variability in θ_s observed on T1, especially in the layered soils of the fluvent. Thus, Θ_e was calculated using observed θ maxima during periods when WTE (measured in well T1-W1) was above probe installation elevations. Fit parameters, θ_s values used for calculation of Θ_e, and C_{eff} values for each time series are summarized in Table 5. For soils that exhibited a wide range of θ values (high and middle elevation sandy soils on the hydric hammock), the model did a good job of predicting soil moisture based on SWE ($0.64 \le C_{eff} \le 0.82$). For deeper sandy soils, which were below the water table for long periods, and surface soils of the lower floodplain, which rarely dry out, the sigmoid model performed fairly ($0.33 \le C_{eff} \le 0.78$). For the lowest elevation soils of the floodplain, which remained saturated for the entire study period, the two-parameter model is simplified to the equation $\Theta_e = 1$, independent of SWE (with a corresponding $C_{eff} = 1.0$).

Table 5. Saturated soil moisture content used to calculate effective soil moisture and parameters fit to Eq. [4] to model effective soil moisture as a function of surface water elevation on Transect 1.

Probe	θ_s†	*a*	*b*	C_{eff}‡
T1-60 (3.90 m)	0.40	3.91	0.24	0.64
T1-60 (3.80 m)	0.35	3.63	0.15	0.72
T1-60 (3.60 m)	0.28	3.33	0.06	0.78
T1-50 (3.71 m)	0.34	3.63	0.16	0.77
T1-50 (3.41 m)	0.35	3.41	0.07	0.82
T1-50 (3.06 m)	0.33	3.26	0.06	0.65
T1-30 (2.76 m)	0.74	3.01	0.12	0.54
T1-30 (2.51 m)	0.74	2.75	0.12	0.33
T1-30 (2.21 m)	0.71	—§	—§	1.00
T1-1 (2.71 m)	0.80	3.13	0.09	0.51
T1-1 (2.46 m)	0.75	2.76	0.12	0.34
T1-1 (2.24 m)	0.63	—§	—§	1.00

† θ_s, saturated soil moisture content.

‡ C_{eff}, Nash–Sutcliffe coefficient of efficiency, used to assess model goodness-of-fit.

§ For permanently flooded soils, the model for effective soil moisture (Θ_e) simplifies to $\Theta_e = 1$, with $C_{eff} = 1.0$.

Although consideration of rain, ET, antecedent moisture conditions, and surface topography would improve the model's predictive ability, this simplified relationship is useful for evaluating the effects of river management on θ profiles because MFL and restoration scenarios are based on flow at Lainhart Dam (calculated from SWE). We also recognize that underlying this Θ_e–SWE model is the fundamental relationship describing θ as a function of soil water pressure head (ψ) (e.g., Brooks and Corey, 1964; van Genuchten, 1980). Under relatively hydrostatic conditions (i.e., no inflow, outflow, or redistribution of soil water above the water table), ψ can be estimated as the distance to the water table (Skaggs, 1991). Because SWE and WTE at T1 are tightly coupled (overall r^2 = 0.88), directly linking θ to SWE is consistent with these fundamental relationships.

In general, Eq. [4] yielded increasingly dry soil moisture profiles with increasing elevation. To expand the applicability of this model to the remainder of the floodplain at T1, trends between *a* and *b* parameters and probe installation elevations and distances from the river were examined. Plotting *a* and *b* versus probe installation elevation and fitting a third-order polynomial yielded good results (r^2 = 0.96 and 0.78 for *a* and *b*, respectively), with:

$$a = 1.425x^3 - 13.421x^2 + 42.241x - 41.171 \quad [6]$$

$$b = 0.248x^3 - 2.112x^2 + 5.873x - 5.249 \quad [7]$$

where *x* is topographical elevation (m, NGVD29). Overall C_{eff} for the 12 Θ_e time series using the approximations in Eq. [6] and [7] was 0.83. Including elevation and distance from the river as variables for fitting the parameters in Eq. [4] yielded a better fit (third-order polynomial in elevation and distance; r^2 of 0.99 and 0.96 for *a* and *b* parameters, respectively; overall C_{eff} = 0.91), as might be expected based on the effects of surface topography, shape of the water table, and soil heterogeneity.

To assess the added benefit of the more complex model based on elevation and distance from the river, both models were used to estimate Θ_e at the soil surface, 10 cm below ground surface, and 50 cm below ground surface at four distances from the river (60, 50, 30, and 1 m) under three flow scenarios in the MFL and restoration plan. Differences in model results were generally small (average absolute difference of 4.6, 4.3, and 5.4% at the three depths). The largest differences were seen 50 m from the river (Fig. 3a), where elevation changes abruptly. Ultimately, the simpler model was preferred because it had fewer parameters, performed adequately, and is consistent with the underlying soil physics (assuming a relatively flat water table over the length of T1).

A nomograph describing Θ_e at T1 was developed based on the simpler model (Fig. 7), which can be used to estimate moisture profiles across the floodplain under different river management scenarios. For example, the MFL of 1 $m^3\ s^{-1}$ corresponds to SWE of 3.31 m at Lainhart Dam (vertical dashed line in Fig. 7). This yields a Θ_e profile ranging from 0.06 on top of the hydric hammock (on the 3.9 m curve) to 1.00 in the consistently flooded soils of the floodplain (on the < 2.5 m curve), with Θ_e = 0.86 at the lower floodplain soil surface (average elevation 2.81 m; black circle in Fig. 7). Specific moisture thresholds for bald cypress seed germination success have not been identified; however, assuming that a value of $\Theta_e \ge 0.90$ corresponds to "moist" organic soil conditions, ideal bald cypress seedling germination conditions at the soil surface would require maintenance of SWE at Lainhart Dam between 3.35 and 3.52 m, above which the floodplain is generally inundated (SFWMD, 2006). The restoration plan calls for a variable dry season flow between 1.42 and 3.11 $m^3\ s^{-1}$, which corresponds to SWE of 3.36 to 3.52 m at Lainhart Dam (dark gray shaded area in Fig. 7). Thus, dry season restoration flows should provide good conditions for bald cypress seedling germination in the floodplain, whereas the MFL is likely insufficient to maintain the bald cypress ecosystem at T1.

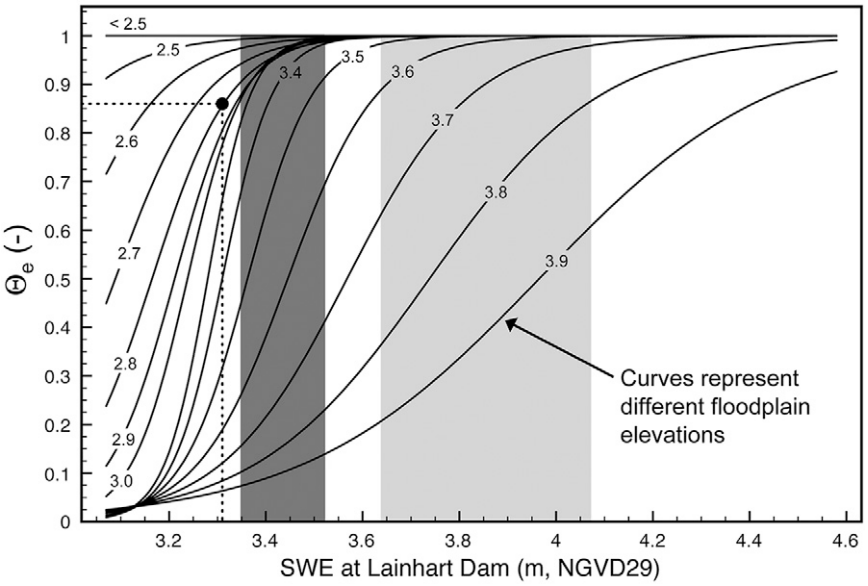

Fig. 7. Nomograph for estimating effective soil moisture (Θ_e) profiles on Transect 1 based on surface water elevation (SWE) at Lainhart Dam and soil elevation (m, NGVD29; labeled on curves). Filled circle represents Θ_e at the average soil surface elevation (2.81 m) in the lower floodplain under the minimum flow level (SWE = 3.31 m). Dark shaded area corresponds to dry season flow levels (3.35 ≤ SWE ≤ 3.52), and light shaded area corresponds to wet season floods with 1- to 2-yr return interval (3.64 ≤ SWE ≤ 4.07), as identified in the restoration plan.

Downstream Transect 7

Due to daily tidal inundation, θ was relatively consistent over the study period, with very little variation regardless of elevation or distance from the river. However, inspection of θ data from the highest elevation (i.e., shallowest) probe revealed a correlation between θ and SWE. Figure 8 shows a 6-d time series of soil moisture for the highest elevation probe on T7 (T7-135; 0.37 m). Fourier smoothing of 30-min θ data and 15-min SWE data to 6-h time series reveals that when mean SWE is above the probe elevation, θ and SWE are tightly coupled, with coinciding peaks and valleys corresponding to low and high tides. When mean tide drops below probe elevation, this relationship breaks down, and the surface soil continues to dry (though slightly).

The total range of variation in soil moisture observed at T7 is small (a change of 1.24% between saturation and "drawdown" moisture contents in Fig. 8) and is unlikely to affect seed germination or seedling survival at this transect. Instead, germination and seedling survival here are likely more limited by tidal inundation range and periods of high SWEC and σ_w.

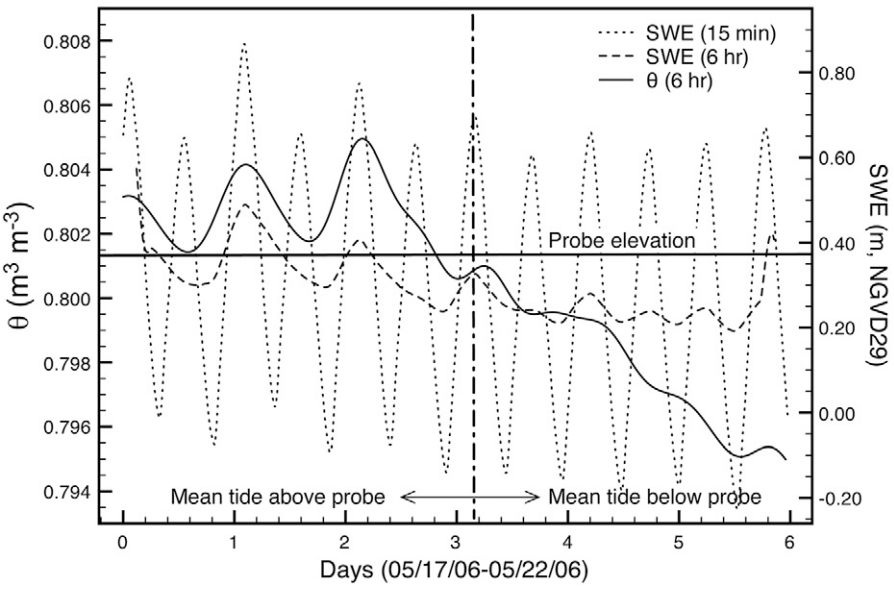

Fig. 8. Relationship between soil moisture (θ) and surface water elevation (SWE) in the highest elevation (i.e., shallowest) probe on downstream, tidally influenced Transect 7 over 6 d in May 2006. Changes in θ were small (~1%) and tightly coupled with SWE but only when mean tide was above probe elevation.

Surface Water, Groundwater, and Porewater Electrical Conductivity Relationships

A basic premise of the restoration plan is that supplying additional freshwater flow over Lainhart Dam will reduce SWEC downstream, reducing the extent of saltwater intrusion. Plotting SWE at Lainhart dam against SWEC at RK 14.6 confirms this relationship (Fig. 9). The regression equation developed for downstream salinity based on total freshwater flow to the NW Fork (eq. [5]; SFWMD, 2006) did a fair job of representing the observed data from 2004 to 2008 at this location (C_{eff} = 0.42; r^2 = 0.51). Re-fitting the parameters in Eq. [5] using 4 yr of observed data yielded only slightly better results (C_{eff} = 0.55; r^2 = 0.54). This is because SWEC at RK 14.6 was highly variable when total flow to the NW Fork was less than ~2.7 $m^3 s^{-1}$. As noted in SFWMD (2006), freshwater flow was identified as the most important variable affecting downstream SWEC, but daily variations in tide, wind speed and direction, groundwater fluxes, and precipitation and ET also drive downstream SWEC.

Accepting this variability, it is useful to identify the specific management thresholds required to maintain SWEC below the 0.3125 S m^{-1} threshold, again using SWE at Lainhart Dam as the primary controllable variable in the system. Based on the range of measurements observed during this study, SWE at Lainhart dam should be maintained ≥3.40 m to keep SWEC at RK 14.6 below the threshold 100% of the time, while maintaining SWE at 3.31 m would prevent 95% of all salinity events exceeding 0.3125 S m^{-1} (vertical dashed line in Fig. 9). Surface water elevation of 3.31 m at Lainhart Dam corresponds to a freshwater flow of ~1.0 $m^3 s^{-1}$, which is the MFL selected for the NW Fork of the Loxahatchee River. The restoration plan identifies a mean monthly resto-

ration flow of 1.95 $m^3 s^{-1}$, which corresponds to a SWE of 3.42 m. Thus, despite only fair agreement between earlier modeling results and observed data, flows identified in the MFL and Restoration Plan would have been sufficient to maintain SWEC at RK 14.6 below 0.3125 S m^{-1} 95 and 100% of the time, respectively, during this 4-yr study.

Next, σ_w in the floodplain was compared with SWEC in the river channel and GWEC at each transect. At upstream T1, σ_w was consistently 2 to 3 times SWEC and GWEC; however, no clear relationships between σ_w and SWE, SWEC, WTE, or GWEC series were apparent. At T7, there was a lag between SWEC and σ_w time series. These delays ranged between 22 and 90 d and increased with depth and distance from the river. Peaks in σ_w were also more persistent than those in SWEC, lasting as much as 7 mo after SWEC had returned to lower levels (Fig. 5e–5f). These σ_w dynamics suggest that salts move from the river into the floodplain soils as a diffusive wave at T7. During wet seasons and on the rising limb of σ_w peaks, σ_w was highest in surface soils and decreased with depth at all locations. This trend was reversed on the falling limb of σ_w peaks when the deeper soils lagged behind (e.g., Fig. 5f).

Because soils at T7 are consistently at or near saturation, high EC surface water inundating the floodplain causes little advective flux of salts into the soil. Instead, salts in daily tidal floodwaters diffuse into the porewater of saturated surface soils and then move downward in the soil profile as a diffusive front. This pattern is reversed when SWEC decreases and tidal floodwaters flush salts from the system, reducing σ_w from the top down. This mechanism also explains the lag between SWEC and σ_w series.

Despite this lag and the persistence of high σ_w after SWEC decreases, some trends between the two series at T7 are apparent. Most importantly, SWEC peaks at RK 14.6 were always greater than the corresponding σ_w peaks, indicating that restoration scenarios designed to maintain SWEC in the river channel below the 0.3125 S m^{-1} threshold also prevent σ_w exceedances in the floodplain. The spatial relationship between SWEC and σ_w across the floodplain at T7 is illustrated in Fig. 10, which shows the average, minimum, and maximum ratios between SWEC and σ_w peaks for high, middle, and low elevation measurement locations. In general, the σ_w/SWEC ratio was high close to the river and decreased with distance, although the highest ratios were observed slightly away (25 m) from the river. This agrees with observations from other tidal systems (e.g., Adams, 1963; Niering and Warren, 1980), where greater high tide flushing and low tide drainage were hypothesized to cause lower salinities at the channel edge than in the interior. At the extremes, σ_w peaks in the floodplain reached a maximum of 63% of the SWEC peaks observed at RK 14.6 (in the highest elevation soils at station T7-25; Fig. 10a) and less than 1% of SWEC (in the lowest elevation soils at station T7-135; Fig. 10c). Although these ranges are wide, they can be used to determine the range of probable σ_w peaks in the floodplain based on measured or modeled SWEC at RK 14.6.

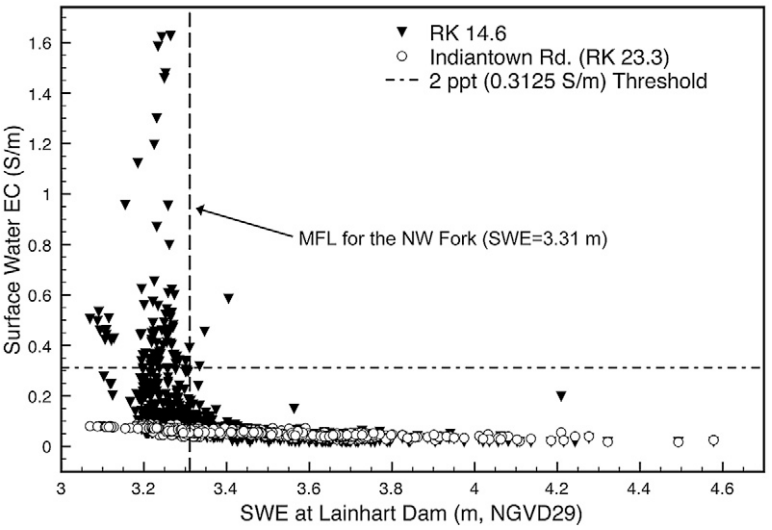

Fig. 9. Surface water electrical conductivity (SWEC) at Indiantown Road (near Transect 1) and river kilometer (RK) 14.6 (near Transect 7) versus surface water elevation (SWE) at Lainhart Dam. Downstream SWEC is variable below SWE of 3.4 m; however, 95% of SWEC exceedances above the 2 ppt (0.3125 S m^{-1}) threshold for maintenance of bald cypress health occur when SWE ≤ 3.31 (vertical dashed line).

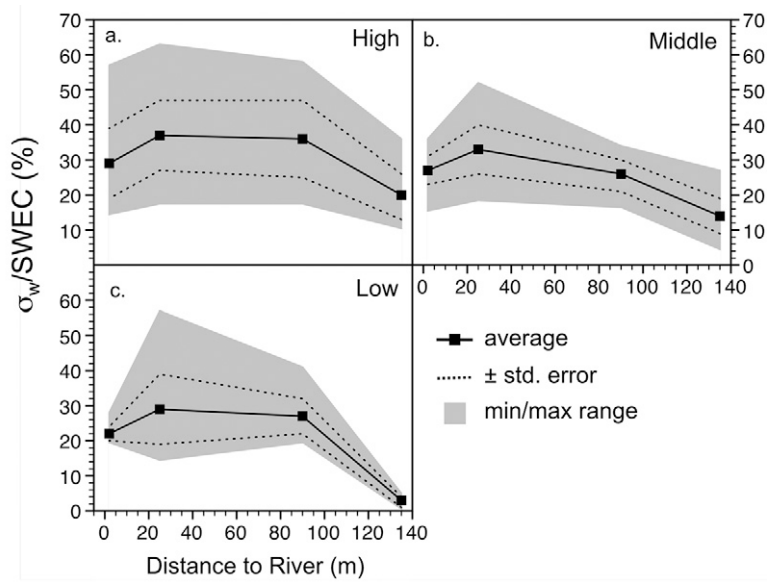

Fig. 10. Ratio of surface water electrical conductivity (SWEC) peaks reached in porewater electrical conductivity (σ_w) in (a) high, (b) middle, and (c) low elevation measurement locations on Transect 7, calculated from daily average data. Ratios are <100% at all depths and distances, indicating that restoration scenarios that succeed in maintaining SWEC below 0.3125 S m^{-1} will also maintain $\sigma_w \leq 0.3125$ S m^{-1} in the floodplain vadose zone.

Summary and Conclusions

Bald cypress floodplain swamp and hydric hammock have been identified as VECs in the Northwest Fork of the Loxahatchee River, which has suffered from increased salinity and reduced hydroperiod due to hydrologic modifications in the watershed. The NW Fork has been the focus of intensive data collection and modeling efforts aimed at developing ecosystem restora-

tion scenarios to benefit VECs, but previous studies had overlooked hydrological conditions in the floodplain vadose zone. To meet the goal of protecting and restoring this ecosystem, this 4-yr study investigated soil moisture (θ) and soil porewater electrical conductivity (σ_w) dynamics in the floodplain of the Loxahatchee River at two transects: an upstream, freshwater transect dominated by bald cypress (T1) and a downstream, transitionally tidal transect with a mix of freshwater and salt-tolerant species (T7). These data were complemented by collocated surface water and groundwater stage and salinity and meteorological data.

The study provides a quantitative validation of our qualitative expectations that complex interactions of rainfall, surface water, and groundwater dominate the dynamics of θ and σ_w in coastal wetlands and that the hydraulic structure effects in these areas propagate in the floodplain vadose zone some distance from the structure. In particular, upstream σ_w rarely exceeded tolerance thresholds for bald cypress but did so more frequently (and for longer duration) in some downstream areas. These data provide a better explanation for the observed spatial patterns of floodplain vegetation than surface water or groundwater data, reinforcing the importance of monitoring in the vadose zone.

Additionally, mechanistic frameworks using conditional modeling approaches can benefit from an improved understanding of which variables are most important within the floodplain. For instance, dynamic θ conditions in the upstream riverine floodplain were successfully modeled as a function of SWE, whereas θ variation in the downstream tidal floodplain was small (though twice daily tidal inundation might limit seed germination and seedling survival to isolated microtopographic points). The θ and σ_w relationships drawn in the study allow us to assess the likely impacts of restoration and management scenarios on the ecological communities in the floodplain of the Loxahatchee River. For example, the proposed restoration flow scenario (which was developed based on floodplain inundation and downstream surface water quality performance measures) will provide good θ conditions for bald cypress seed germination in the riverine floodplain at T1 during the dry season and maintain σ_w in the soil profile below the bald cypress tolerance threshold at T7.

The field and analytical methods used here can be applied to other locations where restoration of floodplain ecosystems depends on hydrological conditions in the vadose zone. These efforts would be further improved by species-specific studies of moisture requirements for seed germination and studies on the effects of variable tidal inundation on the seeds and seedlings of important floodplain species. Continued monitoring of river and floodplain hydrology and vegetation in the Loxahatchee River are important to determine whether the restoration flow scenario is achieving the goal of protecting and restoring VECs.

Acknowledgments

This work was funded in part by the South Florida Water Management District. D. Kaplan and R. Muñoz-Carpena thank Paul Lane for his tireless support in the field and laboratory and Amanda Mortl for providing the foundation for this work. Field assistance from J. Freeman, R. Freeman, F. Tais Kolln, S. Muller, D. Preston, A. Ritter, J. Schroeder, K. VanDerlinden, C. Yu, Z. Zajac, and M. Zamora was greatly appreciated. The authors also thank C. Conrad (SFWMD); D.A. Arrington and D. Sabine (LRD); and C. Price and E. Guevara (USGS) for providing elevation, GIS, hydrology, and water quality data.

References

Abrol, I.P., J.S.P. Yadav, and F.I. Massoud. 1988. Salt affected soils and their management. FAO Soils Bulletin 39. Food and Agriculture Organization, United Nations, Rome, Italy.

Adams, D.A. 1963. Factors influencing vascular plant zonation in North Carolina salt marshes. Ecology 44:445–456.

Alexander, T.R., and A.G. Crook. 1975. Recent and long-term vegetation changes and patterns in south Florida, Appendix G, Part I, South Florida Ecological Study. Univ. of Miami, Coral Gables, FL.

Allen, J.A., J.L. Chambers, and D. McKiney. 1994. Intraspecific variation in the response of *Taxodium distichum* seedlings to salinity. For. Ecol. Manage. 70:203–214.

Allen, J.A., S.R. Pezeshki, and J.L. Chambers. 1996. Interaction of flooding and salinity on baldcypress (*Taxodium distichum*). Tree Physiol. 16:307–313.

Bechtol, V., and L. Laurian. 2005. Restoring straightened rivers for sustainable flood mitigation. Disaster Prevent. Manage. 14:6–19.

Brooks, R.H., and A.T. Corey. 1964. Hydraulic properties of porous media: Hydrology Paper 3. Colorado State Univ., Fort Collins, CO.

Burkett, V., J.O. Codignotto, D.L. Forbes, N. Mimura, R.J. Beamish, and V. Ittekkot. 2001. Coastal Zones and Marine Ecosystems. *In* J. McCarthy, O. Canziani, N. Leary, D. Dokken, and K. White (ed.) Climate change 2001: impacts, adaptation & vulnerability. Contribution of Working Group II to the Third Assessment Report of the Intergovernmental Panel on Climate Change (IPCC). Cambridge Univ. Press, New York.

Burns, R.M., and B.H. Honkala. 1990. Silvics of North America. USDA Forest Serv. Agric. Handbook 654. USDA Forest Serv., Washington, DC.

Campbell, J.E. 1990. Dielectric properties and influence of conductivity in soils at one to fifty Megahertz. Soil Sci. Soc. Am. J. 54:332–341.

Chabrek, R.H. 1972. Vegetation, water and soil characteristics of the Louisiana coastal region. Bull 614. Louisiana State Univ., Baton Rouge.

Conner, W.H. 1988. Natural and artificial regeneration of baldcypress (*Taxodium distichum* [L.] Rich.) in the Barataria and Lake Verret basins of Louisiana. Ph.D. diss. Louisiana State Univ., Baton Rouge, LA.

Conner, W.H., and J.R. Toliver. 1987. Vexar seedling protectors did not reduce nutria damage to planted baldcypress seedlings. USDA Forest Serv. Tree Planter's Notes 38:26–29.

Conner, W.H., J.R. Toliver, and F.H. Sklar. 1986. Natural regeneration of baldcypress [*Taxodium distichum* (L.) Rich.] in a Louisiana swamp. For. Ecol. Manage. 14:305–317.

Costanza, R., D.R. Arge, R. De Groot, S. Ferber, M. Grasso, B. Hannon, K. Limberg, S. Naeem, R.V. O'Neill, and J. Paruello. 1997. The value of the world's ecosystems services and natural capital. Nature 387:253–260.

Darst, M.R., and H.M. Light. 2008. Drier forest composition associated with hydrologic change in the Apalachicola River Floodplain, Florida. USGS Scientific Investigations Report 2008–5062.

Day, R.H., T.W. Doyle, and R.O. Draugelis-Dale. 2006. Interactive effects of substrate, hydroperiod, and nutrients on seedling growth of *Salix nigra* and *Taxodium distichum*. Environ. Exp. Bot. 55:163–174.

DeLaune, R.D., J.A. Nyman, and W.H. Patrick, Jr. 1994. Peat collapse, ponding and wetland loss in a rapidly submerging coastal marsh. J. Coast. Res. 10:1021–1030.

Dent, R.C. 1997. Rainfall observations in the Loxahatchee River watershed. Loxahatchee River District, Jupiter, FL.

Earles, J.M., 1975. Forest statistics for Louisiana Parishes. USDA For. Sci. Res. Bul. SO-52.

Flynn, K.M., K.L. McKee, and I.A. Mendelssohn. 1995. Recovery of freshwater marsh vegetation after a saltwater intrusion event. Oecologia 103:63–72.

Fowells, H.A. 1965. Silvics of forest trees of the United States. USDA Forest Serv. Agric. Handbook 271. USDA Forest Serv., Washington, DC.

General Land Office. 1855. Surveyor field notes from 1855 survey of the Jupiter/Loxahatchee River area. Available at http://www.labins.org (verified 5 July 2010). Labins, Tallahassee, FL.

Hilhorst, M. 2000. A pore water conductivity sensor. Soil Sci. Soc. Am. J. 64:1922–1925.

Holman, I.P., and K.M. Hiscock. 1998. Land drainage and saline intrusion in the coastal marshes of northeast Norfolk. Q J Eng. Geol. Hydrogeol. 31:47–62.

Johnson, J.W. 2008. United States Water Law: An introduction. Taylor &

Francis, New York.
Johnson, R.G. 1997. Climate control requires a dam at the Strait of Gibraltar. EOS 78:280–281.
Jung, M., T.P. Burt, and P.D. Bates. 2004. Toward a conceptual model of floodplain water table response. Water Resour. Res. 40:9.1–9.13.
Knighton, A.D., K. Mills, and C.D. Woodroffe. 1991. Tidal creek extension and saltwater intrusion in northern Australia. Geology 19:831–834.
Leyer, I. 2005. Predicting plant species' responses to river regulation: The role of water level fluctuations. J. Appl. Ecol. 42:239–250.
Liu, G., Y. Li, R. Muñoz-Carpena, M. Hedgepeth, and Y. Wan. 2006. Effects of salinity and flooding on growth of Bald Cypress (*Taxodium distichum* [L.] Rich.). *In* Abstracts, Intl. Ann. Joint Meet., Am. Soc. Agron., Crop Sci. Soc Am., and Soil Sci. Soc. Am., Indianapolis, IN. 12–16 Nov. 2006.
Liu, W., M. Hsu, A.Y. Kuo, and M. Li. 2001. Influence of bathymetric changes on hydrodynamics and salt intrusion in estuarine system. J. Am. Water Resour. Assoc. 37:1405–1419.
McCarthy, J.J, O.F. Canziani, N.A. Leary, D.J. Dokken, and K.S. White (eds.). 2001. Climate change 2001. Impacts, adaptation and vulnerability. Contribution of Working Group II to the Third Assessment Report of the Intergovernmental Panel on Climate Change. Cambridge Univ. Press, New York.
McPherson, B.F. 1981. The cypress forest community in the tidal Loxahatchee River Estuary: Distribution, tree stress, and salinity. Internal USGS Report. USGS, Ft. Lauderdale, FL.
Melloul, A., and L. Goldenberg. 1997. Monitoring of seawater intrusion in coastal aquifers: Basics and local concerns. J. Environ. Manage. 51:73–86.
Michener, W.K., E.R. Blood, K.L. Bildstein, M.M. Brinson, and L.R. Gardner. 1997. Climate change, hurricanes and tropical storms and rising sea-level in coastal wetlands. Ecol. Appl. 7:770–801.
Middleton, B.A. 1999. Wetland restoration, flood pulsing and disturbance dynamics. John Wiley & Sons, New York.
Middleton, B.A. 2000. Hydrochory, seed banks, and regeneration dynamics across landscape boundaries in a forested wetland. Plant Ecol. 146:169–184.
Middleton, B.A. 2002. Flood pulsing in wetlands: Restoring the natural hydrological balance. John Wiley & Sons, New York.
Mitsch, W.J., and J.G. Gosselink. 2000. Wetlands. John Wiley & Sons, New York.
Moorhead, K.K., and M.M. Brinson. 1995. Response of wetlands to rising sea level in the lower coastal plain of North Carolina. Ecol. Appl. 5:261.
Mortl, A. 2006. Monitoring soil moisture and soil water salinity in the Loxahatchee floodplain. Masters thesis. University of Florida, Gainesville, FL.
Muñoz-Carpena, R., D. Kaplan, and F.J. Gonzalez. 2008. Groundwater data processing and analysis for the Loxahatchee River basin. Final Project Report to the SFWMD. Univ. of Florida, Gainesville.
Nash, J.E., and J.V. Sutcliffe. 1970. River flow forecasting through conceptual models part I: A discussion of principles. J. Hydrol. 10:282–290.
Neidrauer, C. 2009. Water conditions summary. Available at http://www.sfwmd.gov/portal/page/portal/pg_grp_sfwmd_governingboard/portlet_gb_subtab_presentations_page/tab20092120/3%20%20water%20conditions.pdf (verified 5 July 2010). SFWMD, Operations Control Dep., West Palm Beach, FL.
Nicholls, R.J., F.M.J. Hoozemans, and M. Marchand. 1999. Increasing flood risk and wetland losses due to sea-level rise: Regional and global analyses. Glob. Environ. Change 9:S69–S87.
Niemi, G., D. Wardrop, R. Brooks, S. Anderson, V. Brady, H. Paerl, C. Rakocinski, M. Brouwer, B. Levinson, and M. McDonald. 2004. Rationale for a new generation of indicators for coastal waters. Environ. Health Perspect. 112:979–986.
Niering, W.A., and R.S. Warren. 1980. Vegetation patterns and processes in New England salt marshes. Bioscience 30:301–307.
National Park Service. 2004. The National Wild and Scenic Rivers Program. Available at http://www.rivers.gov/wsr-loxahatchee.html (verified 5 July 2010). National Park Service, Burbank, WA.
Press, W.H., S.A. Teukolsky, W.T. Vitterling, and B.P. Flannery. 1993. Numerical recipes in C. Cambridge University Press, New York.
Richards, L.A. (ed.) 1954. Saline and alkaline soils. Chapter 2: Determination of the properties of saline and alkali soils. United States Salinity Laboratory, USDA Handbook No. 60, 2nd ed. Washington, DC.
Richardson, C.J., and N.A. Hussain. 2006. Restoring the Garden of Eden: An ecological assessment of the marshes of Iraq. BioScience 56:477–489.
Roberts, R.E., M.Y. Hedgepeth, and T.R. Alexander. 2008. Vegetational responses to saltwater intrusion along the Northwest Fork of the Loxahatchee River within Jonathan Dickinson State Park. Fla. Sci. 71:383–397.
Roberts, R.E., R.O. Woodbury, and J. Popenoe. 2006. Vascular plants of Jonathan Dickinson State Park. Fla. Sci. 69:288–327.
Sadeg, S.A., and N. Karahanogulu. 2001. Numerical assessment of sweater intrusion in the Tripoli region. Environ. Geol. 40:1151–1168.
Salinas, L.M., R.D. DeLaune, and W.H. Patrick, Jr. 1986. Changes occurring along a rapidly submerging coastal area; Louisiana, USA. J. Coast. Res. 2:269–284.
Scruton, D.A., T.C. Anderson, and L.W. King. 1998. Pamehac Brook: A case study of the restoration of a Newfoundland, Canada, river impacted by flow diversion for pulpwood transportation. Aquat. Conserv.: Mar. Freshwat. Ecosyst. 8:145–157.
SFWMD. 2002. Technical Criteria to support development of minimum flow and levels for the Loxahatchee River and estuary. SFWMD, Water Supply Department, Water Resources Management, West Palm Beach, FL.
SFWMD. 2006. Restoration plan for the northwest fork of the Loxahatchee River. SFWMD, Coastal Ecosystems Division, West Palm Beach, FL.
SFWMD. 2009. Riverine and tidal floodplain vegetation of the Loxahatchee River and its major tributaries. SFWMD and FDEP. Coastal Ecosystems Division and Florida Park Service 5th District. West Palm Beach, FL.
Skaggs, W. 1991. Theory of drainage: Saturated flow. BAE 671 course notes. North Carolina State Univ., Raleigh, NC.
Soil Survey Staff. 1981. Soil survey of Martin County area, Florida. USDA Soil Conserv. Serv. Washington, DC.
Sumner, M.E. 2000. Handbook of soil science. CRC Press, New York.
Treasure Coast Regional Planning Council. 1995. Strategic Regional Policy Plan for the Treasure Coast Region, Rule 29K–5.002, Florida Administrative Code. TCRPC, Stuart, FL.
Thompson, R.S., K.H. Anderson, and P.J. Partlein. 1999. Atlas of relations between climatic parameters and distributions of important trees and shrubs in North America. US Geological Survey Professional Papers 1650-A,-B,-C. US Department of Interior, US Geological Survey, Reston, VA.
Thomson, D.M., G.P. Shaffer, and J.A. McCorquodale. 2001. A potential interaction between sea-level rise and global warming: Implications for coastal stability on the Mississippi River Deltaic Plain. Global Planet. Change 32:49–59.
Toth, D.J. 1987. Saltwater Intrusion Study, Phase II. St. Johns River Water Management District, Paltka, FL.
USACE. 1996. Users Guide to RMA2, Version 4.3. USACE, Waterways Experiment Station Hydraulic Laboratory, Vicksburg, MS.
VanArman, J., G.A. Graves, and D.L. Fike. 2005. Loxahatchee watershed conceptual ecological model. Wetlands 25:926–942.
van Genuchten, M. 1980. A closed form equation for predicting the hydraulic conductivity of unsaturated soil. Soil Sci. Soc. Am. J. 44:892–898.
Wang, F.C. 1997. Dynamics of intertidal marshes near shallow estuaries in Louisiana. Wetlands Ecol. Manage. 5:131–143.
Wang, F.C. 1988. Dynamics of saltwater intrusion in coastal channels. J. Geophys. Res. 93:6937–6946.
Wanless, H.R. 1989. The inundation of our coastlines. Sea Front. 35:264–271.
Wicker, K.M., D. Davis, M. DeRouen, and D. Roberts. 1981. Assessment of extent and impact of saltwater intrusion into the wetlands of Tangipahoa Parish, Louisiana. Coastal Environ. Inc., Baton Rouge, LA.
Winn, K., J. Rovis-Hermann, and M. Saynor. 2004. Saltwater intrusion: A natural process. Supervising Scientist Notes, Dep. of the Environment, Water, Heritage and the Arts, Canberra, Australia.